

A Harmonic Cancellation Technique for an Ultrasound Transducer Excited by a Switched-Mode Power Converter

Sai Chun Tang, *Member, IEEE*, and Gregory T. Clement

Abstract—The aim of this study is to evaluate the feasibility of using harmonic cancellation for a therapeutic ultrasound transducer excited by a switched-mode power converter without an additional output filter. A switching waveform without the third harmonic was created by cascading two switched-mode power inverter modules at which their output waveforms were $\pi/3$ phase-shifted from each other. A PSPICE simulation model for the power converter output stage was developed. The simulated results were in good agreement with the measurement. The waveform and harmonic contents of the acoustic pressure generated by a 1-MHz, self-focused piezoelectric transducer with and without harmonic cancellation have been evaluated. Measured results indicated that the acoustic third harmonic-to-fundamental ratio at the focus was small (-48 dB) with harmonic cancellation, compared to that without harmonic cancellation (-20 dB). The measured acoustic levels of the fifth harmonic for both cases with and without harmonic cancellation also were small (-46 dB) compared to the fundamental. This study shows that it is viable to drive a piezoelectric ultrasound transducer using a switched-mode power converter without the requirement of an additional output filter in many high-intensity focused ultrasound (HIFU) applications.

I. INTRODUCTION

SWITCHED-MODE direct current (DC)-to-alternating current (AC) power converters are commonly used for ultrasound piezoelectric transducer excitation [1]–[5] because of their higher power density, high energy efficiency, and low manufacturing cost compared to their linear counterparts. However, without additional filtering circuitry at the power converter output, the harmonics present in the output switching waveform produce undesired acoustic sidelobes in high-intensity focused ultrasound (HIFU) applications [3]. They also incur unnecessary power dissipation from the power converter and the transducer.

In HIFU therapy, acoustic energy is required to be focused at a predetermined target in order to form a focal lesion without damaging the surrounding structure [6], [7]. Practically, a sinusoid or a waveform with low harmonic distortion is used for the ultrasound transducer excitation in order to achieve well-defined shapes of focusing [3] as

the presence of the sidelobes induced by the harmonics can tend to deteriorate the accuracy of focal lesion pattern for therapy.

Among various methods for ultrasound transducer excitation, the radio-frequency (RF) linear amplifier delivers the lowest distortion sinusoidal wave over a wide frequency band. Despite these benefits, drawbacks of high power loss, bulky size, and heavy weight has limited its use in modern ultrasound transducer excitation circuits. Advances in power electronics technology have led to the proposal of using switched-mode power converters for ultrasound transducer excitation [1]–[5]. A switched-mode power converter with a pulse-width-modulation (PWM) technique has been used for generating a high power analog waveform with low harmonic distortion, provided that the switching frequency is at least 10 times of the baseband frequency [2], [8]. For baseband frequencies lower than a few tens of kilohertz, the PWM method provides high-energy efficiency and, therefore, is widely used in state-of-the-art commercial audio amplifier systems. However, for most HIFU applications, the acoustic frequency ranges from a few hundreds of kilohertz to several megahertz. The use of a switched-mode power converter with PWM technique would be a challenge because the switching loss of power MOSFETs, which is directly proportional to the switching frequency, would significantly reduce the amplifier efficiency at switching frequency higher than a few megahertz.

A series resonant converter for driving piezoelectric transducer to reduce the switching loss from the power MOSFETs was proposed [1]. Although resonant power converters, in general, can generate low distortion sinusoidal waveform with high-energy efficiency, its operating frequency range is determined by the output resonant inductor and capacitor (LC) tank and is typically restricted to very narrow band. Moreover, the power MOSFETs in the resonant circuit would suffer from higher voltage and current stresses compared to its nonresonant counterpart.

Recently, a nonresonant power converter has been proposed for ultrasound surgery [3]. A high-quality-factor LC filter was used to attenuate the harmonic components of the square wave generated by the converter. With this method, a high-energy efficiency and low-cost multichannel therapeutic ultrasound system could be realized. Similar to the resonant converter, the output LC filter would restrict the amplifier bandwidth, which limits the choice of the ultrasound transducer and frequency.

Manuscript received June 26, 2007; accepted September 25, 2007. This research was supported by research grant No. U41 RR019703 from the National Institutes of Health.

The authors are with the Brigham and Women's Hospital, Harvard Medical School, Department of Radiology, Boston, MA (e-mail: sct@bwh.harvard.edu).

Digital Object Identifier 10.1109/TUFFC.2008.654

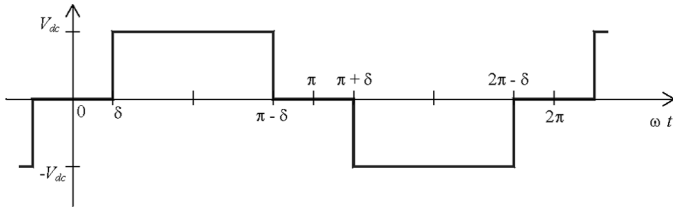


Fig. 1. Switching waveform with third harmonic elimination for transducer excitation.

The present study examines the feasibility of using a switched-mode, nonresonant power converter along with a harmonic cancellation technique for ultrasound transducer excitation. The proposed method does not require an additional output LC filter, and the power converter does not have to operate at resonant mode. Hence, it does not have a frequency limitation imposed by the LC components of the filter or the resonant converter. Our approach is to eliminate the lowest undesired harmonic (third harmonic) by properly selecting the length of the “0” state of a bipolar square wave generated by a switched-mode power converter. Our hypothesis is that higher harmonics of the waveform without the third harmonic would be attenuated naturally by the inherent LC of the converter output transformer and the transducer dielectric capacitance, as well as the mechanical filtering characteristics of the piezoelectric transducer. In this study, a power converter with harmonic cancellation has been designed and developed. A PSPICE (OrCAD 10.5, Cadence Design System Inc., San Jose, CA) model for the power converter output stage has been made. The switching waveforms from the simulation and measurement have been analyzed and compared. The acoustic waveforms and harmonic contents generated by a piezoelectric transducer with and without harmonic cancellation also have been examined and compared. The results in this investigation demonstrate that the proposed harmonic cancellation method offers a viable solution for ultrasound transducer excitation without an additional output filter so as to facilitate the design of wideband ultrasound amplifiers with significantly reduced size, weight, and manufacturing cost.

II. SWITCHING WAVEFORM WITH HARMONIC ELIMINATION

The proposed switching voltage waveform for ultrasound transducer excitation is shown in Fig. 1. By properly selecting the value of δ , the third harmonic can be completely eliminated [9]. Because the waveform is symmetric about its horizontal centerline, it is devoid of even harmonics. The lowest harmonic present in the waveform then will be the fifth harmonic. The formula expressing the n^{th} (where n is odd) harmonic amplitude is:

$$V_{an} = \left| \frac{2V_{dc}}{\pi} \int_{\delta}^{\pi-\delta} \sin(n\omega t) d(\omega t) \right| = \left| \frac{4V_{dc}}{n\pi} \cos(n\delta) \right|, \quad (1)$$

where V_{dc} represents the amplitude of the waveform.

When $\delta = \pi/6$ is chosen, the third harmonic and, in fact, all harmonics of order $3n$ would be eliminated. However, in the case of a regular square wave ($\delta = 0$), the third harmonic amplitude is 33% of the fundamental component. Comparison of the first five odd harmonic amplitudes of the switching waveforms for $\delta = \pi/6$ and $\delta = 0$ (a regular square wave without harmonic elimination) with an amplitude of V_{dc} are tabulated in Table I.

Elimination of lower harmonics (second, third, and fourth harmonics) for piezoelectric transducer excitation has a major advantage in that the undesired higher harmonics (fifth, seventh, eleventh...) could be effectively filtered by the transducer band-pass characteristics and attenuated naturally by the parasitic components at the amplifier output. These include the leakage inductance of the output transformer, the stray capacitance associated with the coaxial cable connected to the transducer, and the inherent dielectric capacitance of the transducer. The higher harmonic contents also can be further attenuated, if necessary, by an output filter with significantly reduced size.

III. EVALUATION OF THE SWITCHING WAVEFORM GENERATED BY A PRACTICAL POWER CONVERTER

A. Power Converter Design

The switching waveform, v_a , with third harmonic cancellation can be achieved by adding two square waves, v_1 and v_2 , with the same amplitude of $V_{dc}/2$, shifted by $\pi/3$ with respect to each other as illustrated in Fig. 2. Based on the Fourier analysis, the previous section has explained that the third harmonic of the switching waveform can be eliminated when $\delta = \pi/6$. Here, from Fig. 2, the absence of the third harmonic in the resultant switching waveform also can be explained by the third harmonic cancellation between the two square waves, as the third harmonic in each of the two square waves has phase shift of π , $3(\pi/3)$, to each other.

Fig. 3 shows a circuit schematic of the power converter that generates the switching waveform with third harmonic cancellation. In the power converter design, each of the square waves is generated by a push-pull inverter module with a center-tapped primary transformer, as an example, although other kinds of topologies, such as a full-bridge inverter, can be adopted for square wave generation [9]. The two inverter modules are identical and connected to the same DC power supply. The turns ratio of the center-tapped primary transformer is 1:1. A pot core with outer-diameter of 26 mm and height of 16 mm, made of 3D3 soft ferrite material from Ferroxcube (Eindhoven, the Netherlands), is used for the transformer. The MOSFETs used in the power converter prototype are IRFR320, from International Rectifier Corporation (El Segundo, CA), in TO-252AA surface mount packages with voltage and current ratings of 400 V and 3.1 A, respectively. The MOS-

TABLE I
HARMONIC VOLTAGE AMPLITUDES OF THE SWITCHING WAVEFORMS WITH AND WITHOUT HARMONIC ELIMINATION.

Harmonic	1st	3rd	5th	7th	9th
Switching waveform with third harmonic elimination ($\delta = \pi/6$)	$1.1 V_{dc}$	0	$0.22 V_{dc}$	$0.16 V_{dc}$	0
Switching waveform without harmonic elimination (square wave, $\delta = 0$)	$1.27 V_{dc}$	$0.42 V_{dc}$	$0.26 V_{dc}$	$0.18 V_{dc}$	$0.14 V_{dc}$

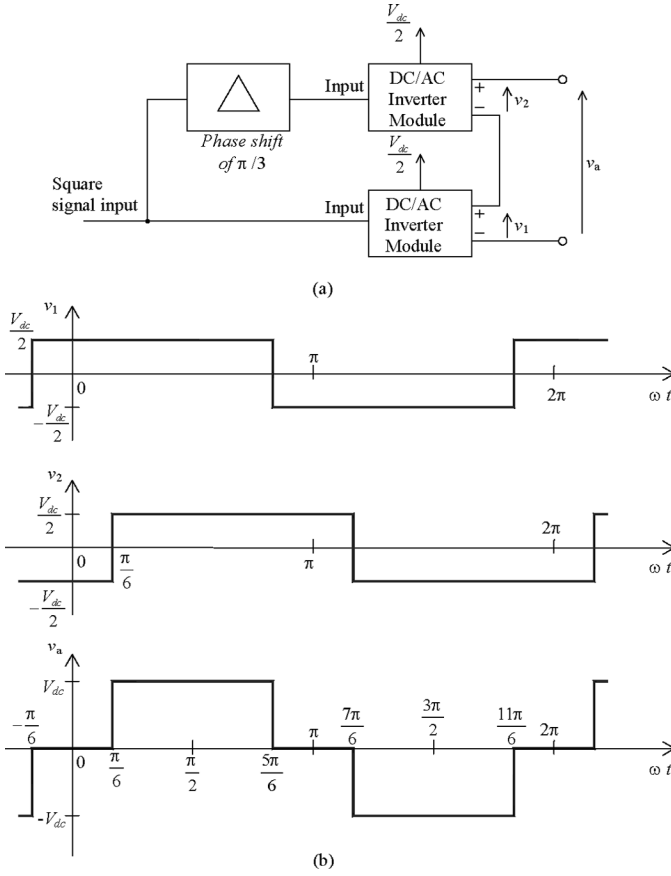


Fig. 2. (a) A block diagram showing the generation of switching waveform with third harmonic cancellation by cascading two power inverter modules with output waveforms phase-shifted by $\pi/3$. (b) The upper two waveforms show the square wave from each of the inverter modules. The bottom waveform shows the resultant waveform by adding the two phase-shifted waveforms.

FETs are driven by dual, high-speed MOSFET drivers with one inverting input, TPS2184 (Texas Instruments Incorporated, Dallas, TX). The gating signal for generating square wave v_1 is directly obtained from the input signal, and that for v_2 is phase-shifted by $\pi/3$ with respect to the input signal.

B. Power Converter Characteristics

The performance of the switching power converter with third harmonic cancellation has been evaluated and compared with its counterpart that generates the regular square wave ($\delta = 0$) by means of experimental measurements and PSPICE simulations. The peak voltage V_{dc} of the output waveform is adjusted to 40 V. The operating frequency of the power converter is set to 1 MHz. A simu-

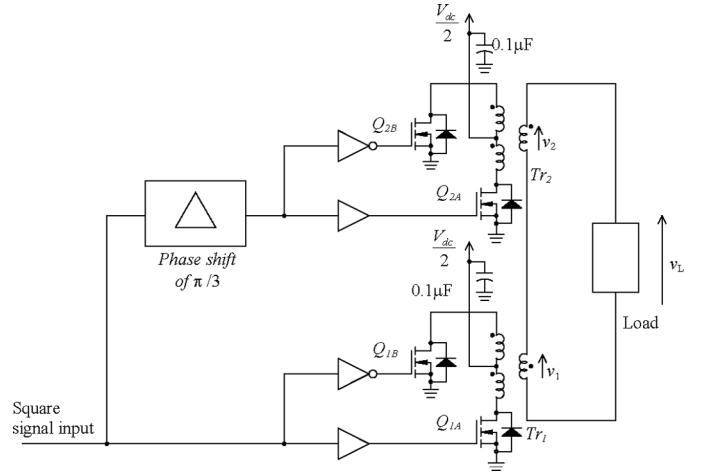


Fig. 3. A circuit schematic of the power converter generating the switching waveform with third harmonic cancellation.

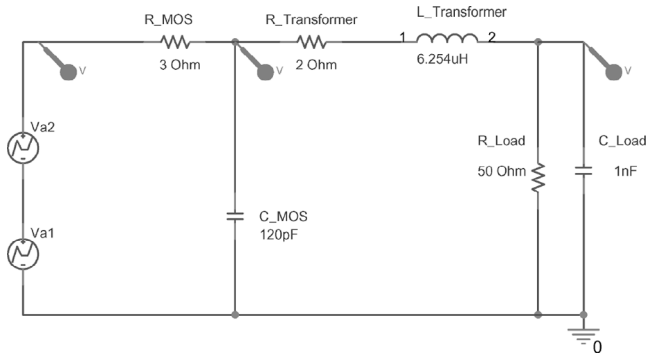


Fig. 4. A simulation model for the power converter shown in Fig. 3.

lation model for the power converter output stage of Fig. 3 has been developed and is shown in Fig. 4. The voltages, v_1 and v_2 , generated by the actual push-pull inverter modules are represented by two ideal square voltages, v_{a1} and v_{a2} , coupled to an output impedance network. The turn-on resistance and drain-to-source capacitance of the MOSFET are modeled by R_MOS and C_MOS in Fig. 4, respectively. The impedance of the output transformers is simplified to a series RL circuit in the model, although a more sophisticated T-model accounting for frequency-dependent core losses can be used for improving the simulation accuracy. The power converter has been evaluated with a resistive load of 50Ω and a parallel RC circuit ($50 \Omega // 1 \text{ nF}$) that the capacitor represents the dielectric capacitance of a piezoelectric ultrasonic transducer.

In the waveform measurement, the regular square voltage, without harmonic cancellation, was generated by the same power converter of Fig. 3, except one of the inverter

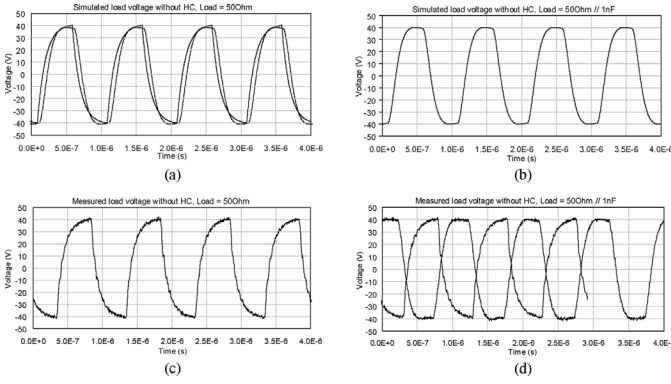


Fig. 5. Simulated and measured output waveforms from the DC/AC power converter without harmonic cancellation. (a) Simulated result with $50\ \Omega$ load. (b) Simulated result with $50\ \Omega/1\ \text{nF}$ load. (c) Measured result with $50\ \Omega$ load. (d) Measured result with $50\ \Omega/1\ \text{nF}$ load.

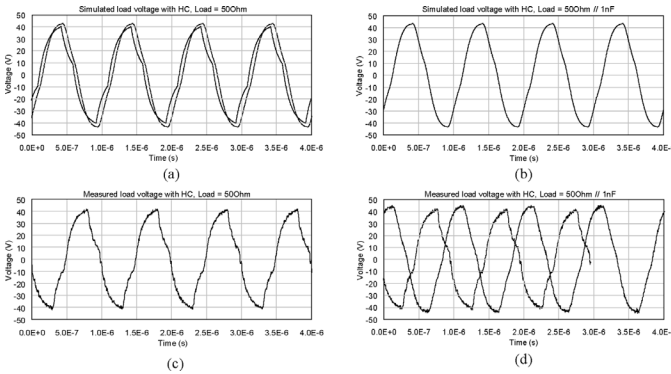


Fig. 6. Simulated and measured output waveforms from the DC/AC power converter with third harmonic cancellation. (a) Simulated result with $50\ \Omega$ load. (b) Simulated result with $50\ \Omega/1\ \text{nF}$ load. (c) Measured result with $50\ \Omega$ load. (d) Measured result with $50\ \Omega/1\ \text{nF}$ load.

modules was disabled and the supply voltage was set to V_{dc} . The PSPICE simulation model for the square wave generator is achieved by setting v_{a1} as the sole voltage source and disconnecting v_{a2} in the model of Fig. 4. The simulated and measured output voltage waveforms from the power converter with and without harmonic cancellation are shown in Figs. 5 and 6, respectively. The sampling rate of the acquired voltage waveforms is 250 megasample per second (MSPS). The measured output voltages are found to be consistent with the PSPICE simulations. For the cases of resistive load, the output voltages change exponentially as the inherent leakage inductance of the output transformer combined with the load resistor acts as an R-L first-order low-pass filter. When a 1 nF capacitor, which represents the dielectric capacitance of a piezoelectric transducer, is added in parallel to the load, the power converter output behaves as a second-order filter, and the waveform is further smoothed. By applying fast Fourier transform (FFT) to the waveforms acquired in Figs. 5 and 6, the harmonic contents of the waveforms from the converter output with the parallel RC load are calcu-

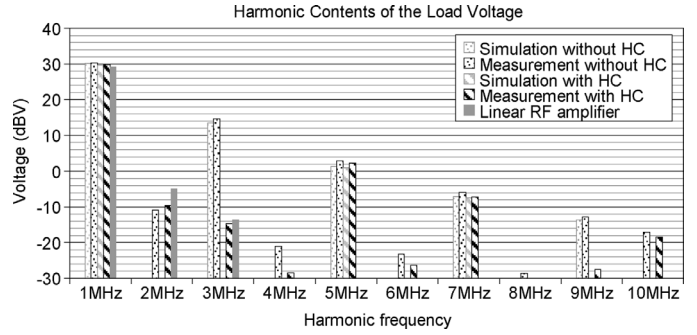


Fig. 7. Simulated and measured harmonic contents from the DC/AC power converter output with and without third harmonic cancellation (HC) loaded with a parallel RC circuit ($50\ \Omega/1\ \text{nF}$), and from the RF linear amplifier.

lated and shown in Fig. 7. The harmonic contents from a class-A RF linear amplifier (240 L, Electronics & Innovation, Rochester, NY) with sinusoidal input from a signal generator (33250A, Agilent Technologies, Santa Clara, CA) also are plotted in Fig. 7 as a control. The y-axis of the plot is in decibel volts, $20 \cdot \log_{10}(V_{peak})$, and the y-minimum is set to $-30\ \text{dBV}$ as the noise floor of about $-35\ \text{dBV}$ to $-32\ \text{dBV}$ was measured from the data acquisition system configured for the measurement. In the practical measurement, very small even harmonics emerge at the output of the converter and the RF linear amplifier. The output voltage second harmonic-to-fundamental ratios from the power converter with and without harmonic cancellation, and from the RF amplifier are $-41\ \text{dB}$, $-40\ \text{dB}$, and $-34\ \text{dB}$, respectively. Also, very small third harmonic-to-fundamental ratios of $-45\ \text{dB}$ and $-43\ \text{dB}$, respectively, at the load voltage from the power converter with harmonic cancellation and from the RF amplifier were measured. However, the measured power levels from the even harmonics and from the third harmonic of the waveform with harmonic cancellation are negligible compared to the corresponding fundamental power. The simulated and measured fifth harmonic-to-fundamental ratios, for the power converter with third harmonic cancellation, are $-29\ \text{dBV}$ and $-28\ \text{dBV}$, respectively. Without harmonic cancellation, the simulated and measured third harmonic-to-fundamental ratios from the power converter output are $-17\ \text{dBV}$ and $-16\ \text{dBV}$, respectively.

IV. POWER CONVERTER LOADED WITH PIEZOELECTRIC TRANSDUCER

A. Transducer Excitation Waveform

The operation of the power converter has been verified with a 1-MHz resonance lead zirconium titanate (PZT) crystal (EBL, East Hartford, CT), with 20-mm diameter, and 40-mm radius of curvature. In order to measure the excitation voltage across the transducer terminals, the transducer was mounted into the wall of a plastic container. The transducer terminals are accessible to a voltage probe on

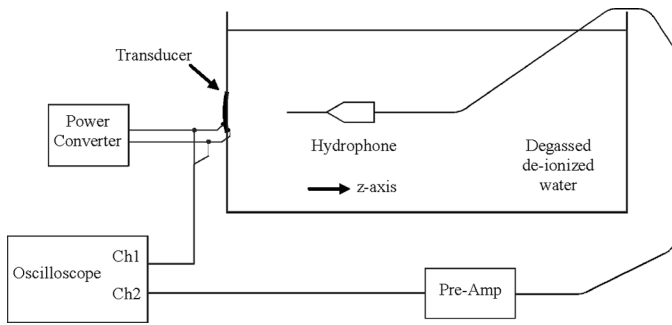


Fig. 8. Experimental setup for transducer excitation and acoustic measurements.

the air side and connected to the power converter output, as shown in Fig. 8. The container was filled with degassed, deionized water during experiment. The measured voltage waveforms across the transducer excited by the power converter without and with harmonic cancellation are shown, respectively, in Fig. 9(a) and (b). The voltage waveform across the transducer excited by the class-A linear amplifier with a sinusoidal input also was captured and is shown in Fig. 9(c) as a control. By applying FFT to the time domain waveforms in Fig. 9, the harmonic contents of the transducer excitations have been calculated and summarized in Fig. 10. Similar to the results with the RC load, the transducer excitation waveform from the RF linear amplifier and power converter with harmonic cancellation exhibits very low third harmonic-to-fundamental contents of -50 dB and -46 dB, respectively, compared to the -15 dB for that without harmonic cancellation. However, a noticeably higher second harmonic voltage was observed at the power source output with the transducer load compared to the RC load. With the transducer load, the second harmonic-to-fundamental ratio from the power converter with and without harmonic cancellation, and from the RF amplifier are -25 dB, -20 dB, and -31 dB, respectively. The substantial increase in the second harmonic amplitude might be attributed to the nonlinearity behavior of the piezoelectric transducer used in the experiment. The measured fourth harmonic-to-fundamental ratio of the excitations from all of the power sources are less than -50 dB. The fifth harmonic-to-fundamental ratio for the power converter with and without third harmonic cancellation are about -32 dB. The fifth harmonic content from the RF amplifier output is less than the noise floor of the waveform acquisition system.

B. Transducer Acoustic Frequency Response

The experimental setup for evaluating the acoustic frequency response of the transducer is illustrated in Fig. 8. A needle hydrophone (Precision Acoustics Ltd., Dorset, UK) with a diameter of 0.2 mm was used to sense the acoustic pressure along the ultrasound propagation axis (z -axis). The scanning distance range is between 20 mm and 100 mm from the transducer, and the step size is set to 0.1 mm. The acoustic frequency response of the

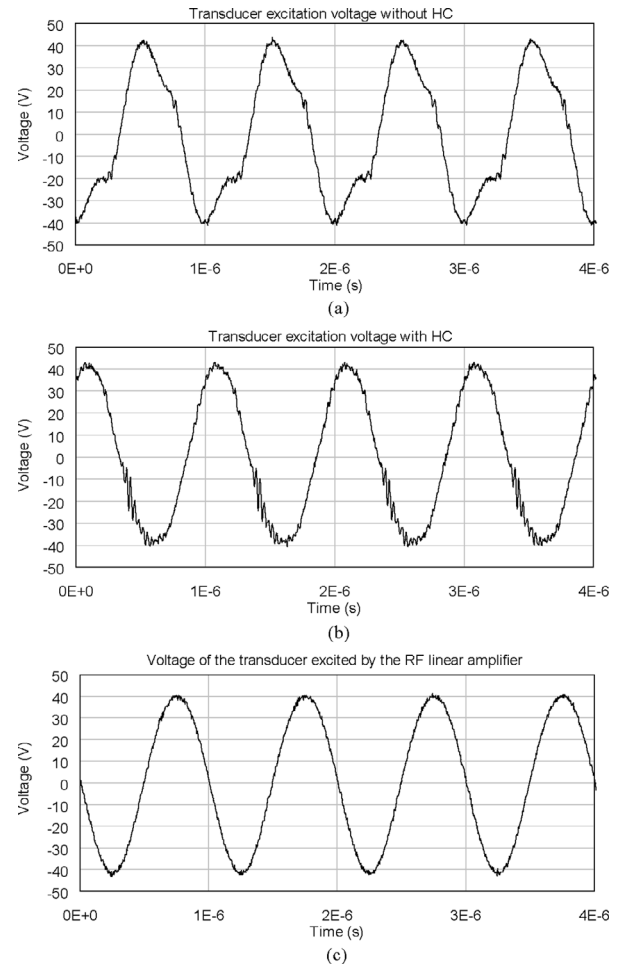


Fig. 9. Measured voltage waveforms of the transducer excited by the power converter. (a) Without and (b) with harmonic cancellation. (c) By the RF linear amplifier.

transducer is characterized by exciting the transducer with a sinusoidal waveform with an amplitude of 40 V at various frequencies between 1 MHz and 5 MHz using a linear power amplifier, and measuring the hydrophone root-mean-square (rms) voltage along the z -axis. The hydrophone voltages, corresponding to the acoustic pressure at the tip of the needle hydrophone versus z -axis are plotted in Fig. 11. A peak hydrophone voltage of 17 mV was measured at the transducer focus ($z = 35$ mm) for the 1-MHz excitation. With excitation frequencies of 2 MHz, 3 MHz, 4 MHz, and 5 MHz, the focal distances shift to 38 mm, 40 mm, 42 mm, and 43 mm. The hydrophone voltage at the focal points are 2 mV, 9.6 mV, 7.6 mV, and 3 mV, respectively.

To minimize counting the effect of the accumulated distortion from the propagation medium on the acoustic pressure waveforms, acoustic pressure measurement as close to the transducer as possible are used for the transducer frequency response investigation. The ratios of the acoustic pressure at $z = 20$ mm from the excitations with 2 MHz, 3 MHz, 4 MHz, and 5 MHz to that with 1 MHz have been calculated from Fig. 11 as -29 dB, -15 dB, -13 dB, and -18 dB, respectively.

TABLE II
MEASURED HARMONIC-TO-FUNDAMENTAL RATIOS OF THE HYDROPHONE VOLTAGE WAVEFORM.¹

Harmonic		2nd	3rd	4th	5th
$z = 20$ mm	Power converter with third harmonic cancellation	-33 dB	-56 dB	-55 dB	-43 dB
	Power converter without harmonic cancellation	-36 dB	-33 dB	-54 dB	-43 dB
	RF linear amplifier	-33 dB	-45 dB	-52 dB	-52 dB
$z = 35$ mm	Power converter with third harmonic cancellation	-25 dB	-48 dB	-57 dB	-46 dB
	Power converter without harmonic cancellation	-26 dB	-20 dB	-45 dB	-42 dB
	RF linear amplifier	-25 dB	-54 dB	-61 dB	-61 dB

¹At $z = 20$ mm and $z = 35$ mm (transducer focus) when the transducer was driven by the power converter with and without harmonic cancellation, and the RF linear amplifier.

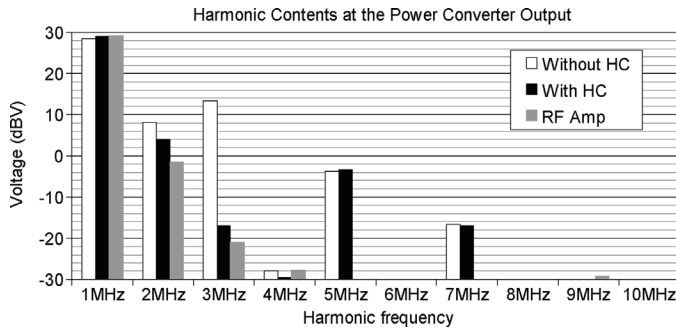


Fig. 10. Harmonic contents of the voltage of the transducer excited by the power converter with and without harmonic cancellation, and by the RF linear amplifier.

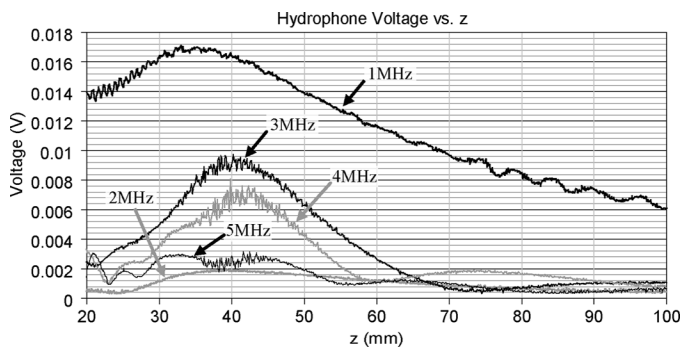
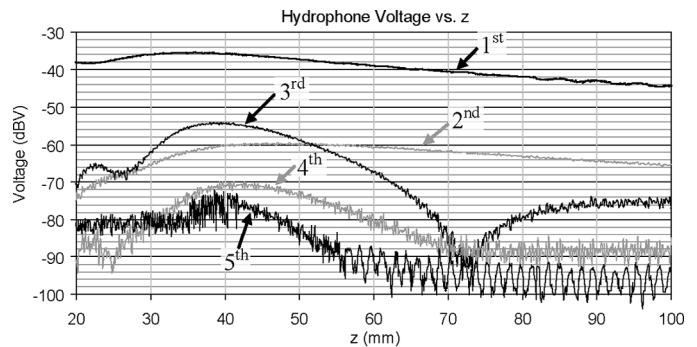


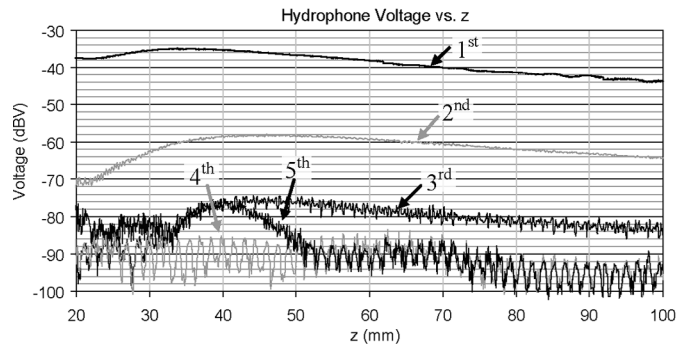
Fig. 11. Hydrophone voltage in root-mean-square (rms) versus distance from the transducer along the propagation axis when the transducer was excited by 40 Vp sinusoidal waveforms at various frequencies of 1 MHz to 5 MHz, respectively.

C. Acoustic Harmonic Contents

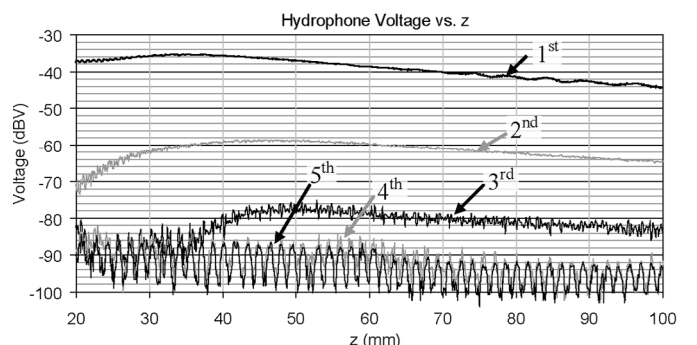
By applying FFT to the measured hydrophone voltage waveform, the harmonic contents of the acoustic wave from the transducer excited by the power converter with and without harmonic cancellation, as well as the RF amplifier along the z -axis, have been obtained, and are shown in Fig. 12. It is noted that the noise floor of the frequency spectrum of the hydrophone voltage measurement is about -110 dBV to -95 dBV, though the y-minimum of the harmonic plot of Fig. 12 is -100 dBV. The acoustic pressure harmonic-to-fundamental ratios at $z = 20$ mm have been derived from the plots of Fig. 12 and are summarized in Table II. With the use of harmonic cancellation,



(a)



(b)



(c)

Fig. 12. Hydrophone harmonic voltage magnitude versus distance from the transducer along the propagation axis when the transducer was driven by waveforms with a voltage amplitude of 40 V and a frequency of 1 MHz from the power converter. (a) Without and (b) with harmonic cancellation. (c) From the RF linear amplifier.

the measured third harmonic-to-fundamental ratio of the acoustic wave at $z = 20$ mm is 23 dB less than that without harmonic cancellation and 11 dB less than that using the RF linear amplifier. The measured fifth harmonic-to-fundamental ratio of the acoustic wave at $z = 20$ mm is less than -40 dB for all of the excitations.

In Fig. 12, the acoustic second harmonic amplitude is noticeable compared to the higher harmonics even though the transducer is excited by a linear amplifier with sinusoidal input, and the second harmonic amplitude is similar for all excitation cases. Consider the linear amplifier excitation as a reference case, the second harmonic-to-fundamental ratio of the transducer excitation voltage is -30 dB (from Fig. 10) and the ratio of the acoustic pressure at $z = 20$ mm with 2 MHz excitation to that with 1 MHz excitation is -29 dB (from Fig. 11). The second harmonic-to-fundamental ratio of the acoustic pressure at $z = 20$ mm should be -59 dB (-30 dB -29 dB) if the transducer is assumed to be linear. However, when the transducer was excited by the voltage at a frequency of 1 MHz and a magnitude of 40 V from the RF amplifier with sinusoidal input, the measured second harmonic-to-fundamental ratio of the acoustic pressure at $z = 20$ mm is -33 dB (from Table II), which is 26 dB higher than the calculated value of -59 dB with the linear assumption. This result implies that the second harmonic acoustic oscillation is attributed to the nonlinearity of the transducer under this operating condition. The second harmonic energy primarily comes from that of the fundamental frequency.

Fig. 13 illustrates the hydrophone voltage waveforms at the transducer focus ($z = 35$ mm) when the transducer was excited by the power converter with and without harmonic cancellation, respectively, and the RF linear amplifier with sinusoidal input. For the case when the transducer was excited by the power converter without harmonic cancellation, the measured acoustic waveform has significantly higher distortion than those with harmonic cancellation and the RF linear amplifier. In terms of harmonic content, as shown in Table II, the acoustic third harmonic-to-fundamental ratio at the transducer focus ($z = 35$ mm) for the case without harmonic cancellation is -20 dB (10%). Those with harmonic cancellation and excited by the RF linear amplifier are -48 dB (0.4%) and -54 dB (0.2%), respectively.

V. DISCUSSION

This study demonstrates a cost-effective method for driving an ultrasound transducer, especially for HIFU applications, using a switched-mode power converter without an additional output filter. Experimental results show that, with using the proposed harmonic cancellation technique, the third harmonic-to-fundamental ratio of the acoustic wave from a piezoelectric ultrasound transducer is negligibly low (-56 dB) compared to that without harmonic cancellation (-33 dB).

The size of a passive filter at the switched-mode power converter output generally is determined by the lowest fre-

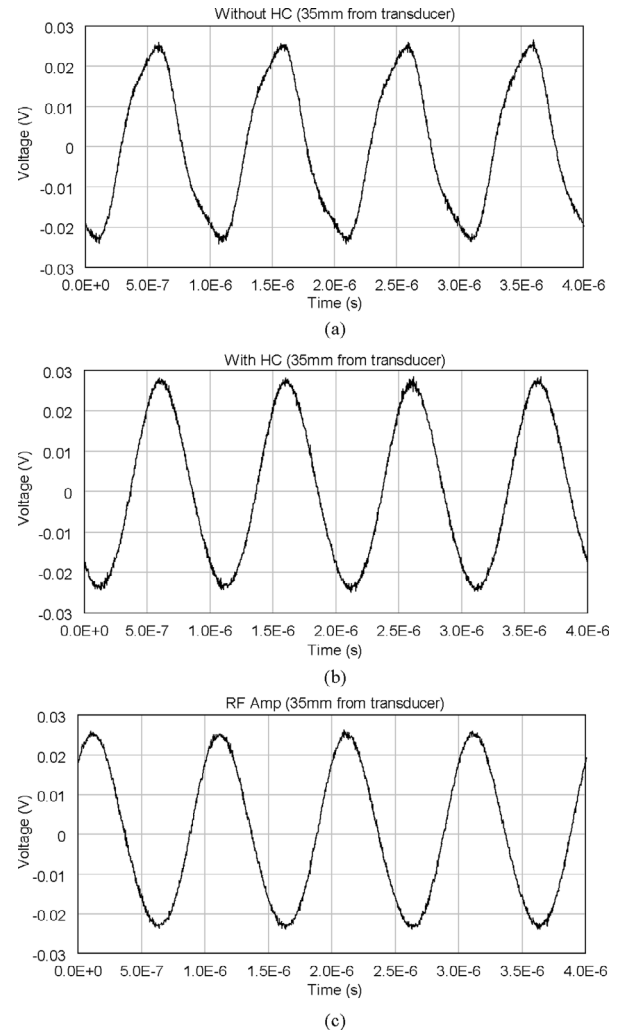


Fig. 13. Voltage waveforms of hydrophone at the transducer focus ($z = 35$ mm) when the transducer was excited by the power converter. (a) Without and (b) with harmonic cancellation. (c) Excited by the RF linear amplifier with sinusoidal input.

quency to be eliminated. Elimination of the third harmonic has major beneficial effects on the size and weight of the filter components because the lower harmonic present at the power converter output then would be the fifth harmonic, provided the output waveform is a square wave with 50% duty cycle. In this study, the fifth harmonic-to-fundamental ratio of the measured acoustic wave from the transducer is very small (< -40 dB at the focus). Elimination of the fifth harmonic may not be necessary for many applications, although a more complicated circuit [9] can be adopted to simultaneously eliminate the third and fifth harmonics. The results of this study represent a significant step toward simplifying ultrasound amplifier design by eliminating the need of an additional output filter that increases the size, weight, power consumption, and manufacturing cost. The output filter also limits the bandwidth of the power amplifier and, therefore, restricts the selection of the ultrasound frequency.

The switching waveform with harmonic cancellation in this study was created by a power converter that is made

of two push-pull power inverter modules generating 50% square wave with $\pi/3$ phase shift from each other. Although a full-bridge power converter also may be used to generate the desired switching waveform, floating gate driver circuits, which significantly increase the circuit complexity and manufacturing cost, are required for the upper leg MOSFETs. The use of two push-pull power inverter modules has the advantages, including, first, that the heat dissipation associated with the power stage can be physically spread over a larger area, reducing the thermal management challenge. Second, because all of the MOSFET source terminals are connected to the common ground, floating or isolated gate drive circuits are not required and considerable cost reduction for the gate drive circuit can be achieved. Third, the control scheme for the modular converter can be much simpler than that for a full-bridge converter as only two square signals shifted by $\pi/3$ are required for the former case, but four individual switching signals are necessary for gating the four MOSFETs in the latter case.

The performance of the power converter developed in this study has been evaluated by PSPICE simulation and experimental measurement. In order to evaluate the performance of the power converter without the influence of distortion effects from the piezoelectric transducer, the power converter was loaded with a $50\ \Omega$ resistor and a parallel RC ($50\ \Omega//1\ \text{nF}$) circuit. Both of the cases with and without harmonic cancellation have been investigated. The measured power converter output voltage waveforms are consistent with the results from the PSPICE simulations. However, in the measurement of harmonic contents, small amounts of even harmonic components were observed at the power converter output due to the timing error made in generating the 50% duty cycle square waveform. A control experiment that used an RF class-A linear amplifier to compare the performance of the power converter has been carried out. It was found that the finite amount of second harmonic observed at the amplifier output was due to the amplifier distortion. The power converter also has been evaluated with a piezoelectric transducer load, and its performance was compared to that of an RF linear amplifier. With transducer load, the output voltage second harmonic is noticeably higher than that with resistive and parallel RC loads. It has been found that the increase in the second harmonic comes from the nonlinearity of the transducer. The measured acoustic second harmonic-to-fundamental ratio near the transducer ($z = 20\ \text{mm}$) is very small (less than $-33\ \text{dB}$, or 2.2%), which is negligible in many HIFU applications and can be reduced further by optimizing the transducer design.

At the focus of the transducer ($z = 35\ \text{mm}$), the acoustic third harmonic content dominates over other harmonics when harmonic cancellation is not applied. However, the use of the harmonic cancellation scheme drastically reduces the acoustic third harmonic-to-fundamental ratio to $-48\ \text{dB}$ at the focus. The acoustic fifth harmonic-to-fundamental ratios at the focus, with and without harmonic cancellation, are negligibly small ($< -40\ \text{dB}$), which

implies that eliminating the third harmonic is sufficient for many HIFU applications.

VI. CONCLUSIONS

This study confirms a fundamental concept that switched-mode power converters with a harmonic cancellation technique can be used for ultrasound transducer excitation, especially for HIFU applications, without the use of an additional filter. A method for eliminating the third harmonic of a switching waveform generated by a switched-mode power converter has been proposed, and its performance has been evaluated by measurement and PSPICE simulation. The simulation results are in good agreement with the measurement. The acoustic pressure waveform created by a piezoelectric transducer with and without using the harmonic cancellation technique was analyzed and compared. It was found that the measured acoustic third harmonic-to-fundamental ratio at the transducer focus for the case with harmonic cancellation ($-48\ \text{dB}$) is much less than that without harmonic cancellation ($-20\ \text{dB}$). Because an additional output LC filter is not necessary when using the proposed technique, it is envisaged that a low-cost, small-size, lightweight, and wideband ultrasound transducer amplifier for many HIFU applications can be realized.

REFERENCES

- [1] P. Fabijanski and R. Lagoda, "Series resonant converter with sandwich-type piezoelectric ceramic transducers," in *Proc. IEEE Int. Conf. Indus. Technol.*, 1996, pp. 252–256.
- [2] K. Agbossou, J.-L. Dion, S. Carignan, M. Abdelkrim, and A. Cheriti, "Class D amplifier for a power piezoelectric load," *IEEE Trans. Ultrason., Ferroelect., Freq. Contr.*, vol. 47, pp. 1036–1041, July 2000.
- [3] T. Hall and C. Cain, "Low cost compact 512 channel therapeutic ultrasound system for transcutaneous ultrasound surgery," in *Proc. 5th Int. Symp. Therapeutic Ultrasound*, May 2006, pp. 445–449.
- [4] T. Suzuki, H. Ikeda, H. Yoshida, and S. Shinohara, "Megasonic transducer drive utilizing MOSFET DC-to-RF inverter with output power of 600 W at 1 MHz," *IEEE Trans. Ind. Electron.*, vol. 46, pp. 1159–1173, Dec. 1999.
- [5] Y. Mizutani, T. Suzuki, J. Ishikawa, H. Ikeda, H. Yoshida, and S. Shinohara, "Single-ended compact MOSFET power inverter with automatic frequency control for maximizing RF output power in megasonic transducer at 3 MHz," in *Proc. IEEE Int. Symp. Circuits Syst.*, 1998, pp. 578–581.
- [6] G. T. Haar, "Ultrasound focal beam surgery," *Ultrasound Med. Biol.*, vol. 21, no. 9, pp. 1089–1100, 1995.
- [7] K. Hynynen, G. T. Clement, N. McDannold, N. Vykhodtseva, R. King, P. J. White, S. Vitek, and F. A. Jolesz, "500-element ultrasound phased array system for noninvasive focal surgery of the brain: A preliminary rabbit study with ex vivo human skulls," *Magn. Resonance Med.*, vol. 52, no. 1, pp. 100–107, July 2004.
- [8] C. Pascual, S. Zukui, P. T. Krein, D. V. Sarwate, P. Midya, and W. J. Roeckner, "High-fidelity PWM inverter for digital audio amplification: Spectral analysis, real-time DSP implementation, and results," *IEEE Trans. Power Electron.*, vol. 18, pp. 473–485, Jan 2003.
- [9] J. G. Kassakian, M. F. Schlecht, and G. C. Verghese, *Principles of Power Electronics*. Reading, MA: Addison-Wesley, pp. 173–179, 1992.



Sai Chun Tang (S'97–M'01) was born in Hong Kong in 1972. He received the B.Eng. degree (with first class honours) and the Ph.D. degree in electronic engineering at City University of Hong Kong in 1997 and 2000, respectively. After he graduated, he worked as a research fellow at the same university. He joined the National University of Ireland, Galway, as a visiting academic in 2001, and then the Laboratory for Electromagnetic and Electronic Systems at Massachusetts Institute of Technology (MIT), Cambridge, MA, as a postdoc in 2002. Since 2004, he has been working at the Focused Ultrasound Laboratory at Brigham and Women's Hospital, Harvard Medical School, Boston, MA, responsible for the developments of ultrasound diagnosis devices and non-invasive treatment systems using an intensive-focused ultrasound beam. His research interests involve high-frequency electromagnetism, low-profile power converter design, and analog electronics.

Dr. Tang is a member of Sigma Xi. He received the Best Paper Award (for posters) at The 16th European Conference on Solid-State Transducers (Eurosensors XVI) in 2002. He won the championship of the Institution of Electrical Engineers (IEE) Hong Kong Younger Member Section Paper Contest 2000, and received the first prize of IEEE HK Section Student Paper Contest'97. He is the inventor/co-inventor of 2 U.S. patents.